Sampling theory inspires quantitative forest ecology: The story of the relascope kernel function

Arne Pommerening [a,*], Hubert Sterba [b], Philip West [c]

[a] *Swedish University of Agricultural Sciences SLU, Faculty of Forest Sciences, Department of Forest Ecology and Management, Skogsmarksgränd 17, SE-901 83 Umeå, Sweden*

[b] *Institute of Forest Growth, Department of Forest and Soil Sciences, BOKU University of Natural Resources and Life Sciences, Peter-Jordan-Straße 82, A-1190 Vienna, Austria*

[c] *Forest Research Centre, Southern Cross University, Lismore, NSW 2480, Australia*

ARTICLE INFO

ABSTRACT

Understanding and modelling plant interactions is an important field in quantitative forest ecology. Many spatially explicit techniques have been devised for shedding light into these processes. One of these methods includes the application of kernel functions, which describe the decay with increasing distance of interaction effects of each plant of a given community on others. In forest inventory, a method referred to as relascope sampling is often applied to collect information on the state and change of tree resources: somewhat unexpectedly, the mathematical principles of this technique have been turned into measures of competition for use in ecological modelling. In this study, we combined methods from quantitative ecology and sampling theory by defining a parameter-parsimonious *relascope kernel function*, thus generalising the concept of individual-tree basal-area factors. By using both relative and absolute growth rates as response variables in the regression we compared the performance of the relascope kernel with an alternative, the exponential kernel function. Our results indicated that the relascope kernel can indeed be applied to both types of growth rates in individual-based models. Using individual-tree basal-area factors, it is even possible to anticipate the performance of the relascope kernel. In most cases the estimation efficiency was greater, when absolute growth rate was the response variable. The exponential kernel was more efficient than the relascope kernel, but at the expense of parameter parsimony and estimation robustness. Our study has shown that simple, parsimonious models, inspired by another field of natural sciences, such as the relascope kernel, can effectively encapsulate the interaction dynamics of forest ecosystems.

1. Introduction

Traditionally, the fields of forest inventory and forest ecology traditionally had little common ground except for the occasional cooperation for work on estimators of ecologically important summary characteristics (Motz et al., 2010; Newton, 2007; Krebs, 1999). Forest inventory has always been more dedicated to estimating the current state of forest resources and associated changes. However, forest ecology, like many other scientific disciplines, largely developed its own sampling theory and procedures to study the dynamics of individuals and populations (Green, 1992), although there were exceptions (see Gregoire et al., 1995; Gregoire and Schabenberger, 1999). This was due to the vast diversity and heterogeneity of forest ecology where sampling

and experimental design often, but not always, overlap (Gregoire, 1998; Newton, 2007; Montgomery, 2013).

One intriguing overlap between forest inventory and forest ecology is an offshoot of *relascope* sampling (also referred to commonly as angle-count or (horizontal) point sampling). The method was originally invented in 1948 by Walter Bitterlich, an Austrian forest scientist, to accelerate and improve the estimation of stand basal area and timber volume in forest stands and was later extended by others (Bitterlich, 1984; Grosenbaugh, 1952; Gregoire and Valentine, 2008). The method is applied also in resource monitoring as part of several national forest inventories (Tomppo et al., 2010). The concept is based on angular measurements made using a small hand-held device referred to as the relascope. The method is used in many parts of the world (e.g West,

---

2015, Section 8.4.2); it has particular advantage where topography is highly variable, since the original relascope device has an automated slope correction ability to avoid bias due to varying slopes.

Interestingly, the relascope idea has been taken up by quantitative forest ecology, particularly in ecological modelling. A common problem in forest modelling is to quantify tree interactions. These interactions are often termed competition, although competition is only a small part of the total interaction between trees. Traditionally, the quantification of competitive effects has been subdivided as (1) the identification of competitors of a given subject tree and (2) the quantification of the competition load, using information of both the competitors and the subject tree (Gadow and Hui, 1999; Burkhart and Tomé, 2012; Weiskittel et al., 2011). Two forms of competitive processes have been identified in forests, *symmetric* and *asymmetric* (e.g Binkley, 2004; Rasmussen and Weiner, 2017; Ouyang et al., 2019; Pommerening and Grabarnik 2019, Section 2.1.1). In the former, trees have competitive effects directly proportional to their sizes. In asymmetric competition, trees have disproportionately large competitive effects with respect to their sizes. For much of the life of a forest, above-ground asymmetric competition for light tends to predominate as taller trees shade smaller but the reverse cannot occur.

Interestingly, researchers in ecology found that aspects of relascope sampling can be used effectively in the identification of competitor trees. Due to its design, the method includes trees in the sample with a probability directly proportional to their sizes (or, formally, to their stem cross-sectional areas at breast height, which generally correlates well with overall tree size). Thus, it tends to prioritise the inclusion of larger trees that are likely to be the asymmetric competitors of other trees (Daniels, 1976; Lorimer, 1983; Tomé and Burkhart, 1989). The choice of the angle used to select trees in a relascope sample influences which trees are included. The larger the angle, the fewer and the larger are the trees that tend to be selected. In practice, these angles are defined through what is known as the *basal area factor* of the sampling device being used (West 2015, Section 8.4.2); this is described fully in Section 2 of this article.

Based on the relascope idea Stöhr (1959) and Spurr (1962) defined an angle summation method that can be used particularly to quantify the competition load suffered by individual trees; it depends on the spatial distribution and relative sizes of neighbouring trees. This approach is headed more in the direction of the second part of studying competitive effects, that is, the actual quantification of competition load. Key to doing this is the derivation of an *individual-tree basal-area factor*; a similar method was used by Rouvinen and Kuuluvainen (1997). McTague (2010) and McTague and Weiskittel (2016) suggested an individual-tree basal-area factor that employs elements of both the original Bitterlich relascope sample and the Spurr method whilst serving as an estimator of basal area and timber volume at the same time. Similar concepts were also suggested by Stage and Ledermann (2008).

In recent years, kernel functions have been increasingly favoured as modern successors to the traditional concept of competition indices that have been used in the past to quantify competition load. Kernel functions are important elements of individual-based models and typically applied for modelling plant interaction and birth processes (Adler, 1996; Schneider et al., 2006; Pommerening and Grabarnik, 2019, Chapter 5). Like basal area factors, they also depend on the size of trees and their distance to other trees or to a sample point. Apart from a solid mathematical foundation and great flexibility, kernel functions offer the benefit of merging the two separate steps involved in the calculation of competitive effects (Pommerening and Maleki, 2014). Therefore the kernel-function concept has the potential to generalise individual-tree basal area factors. Consequently in this paper, we have proposed, analysed and tested a new way of modelling tree interaction by combining the relascope with the kernel-function concept.

The objective of this study was, firstly, to model and analyse a new kernel function which is based on the relascope concept. Secondly, we aimed to analyse and discussed the merits of the new *relascope kernel* and

compared its efficacy when used in modelling both absolute and relative growth rates (of individual-tree stem diameter and basal area) with that of a reference function, the more sophisticated *exponential kernel function* (Pommerening et al., 2011; Pommerening and Maleki, 2014). In the analysis, we used eight different, spatially explicit data sets representing rather different forest types from different parts of the world.

2. Materials and methods

2.1. The concept of the relascope kernel

Consider Fig. 1, where tree *j*, with stem diameter d_j measured at 1.3 m above ground level is located at distance r_j from a point *i*. That point is the centre of a circle of which the circumference passes through the centre of the stem of tree *j*. Consider lines from the point that are tangential to the circumference of the tree stem with an angle between those lines of θ. A tree is included in a point sample if, for a chosen angle θ, it is at or closer to the point than the distance r_j. It then simply follows that

$$r_j = \frac{\frac{d_j}{2}}{\sin\frac{\theta}{2}}. \tag{1}$$

Angle θ depends on a basal-area factor, β^*, defined in Eq. (2). Usually in forest practice, the same factor is employed for all trees in a forest stand; that stand basal area factor is then used to estimate stand basal area from a count of the number of trees included in a sample (West, 2015, section 8.4.2).

$$\beta^* = \frac{\pi \frac{d_j^2}{4}}{\pi r^2} = \left(\frac{d_j}{2\,r}\right)^2 = \sin^2\left(\frac{\theta}{2}\right) \tag{2}$$

This stand basal-area factor, β^*, may be turned into an individual-tree basal-area factor, β_i^*, where r_j is the distance between tree *j* and another tree *i* as:

$$\beta_i^* = \left(\frac{d_j}{2\,r_j}\right)^2 \tag{3}$$

Suppose that a tree with index *i* is referred to hereafter as the *subject tree*. The smaller tree *j* and the further it is from this subject tree *i*, the smaller is the corresponding value of β_i^*. The properties and dependencies of β_i^* are reminiscent of interaction kernels (Adler, 1996; Schneider et al., 2006; Pommerening and Grabarnik, 2019, Chapter 5),
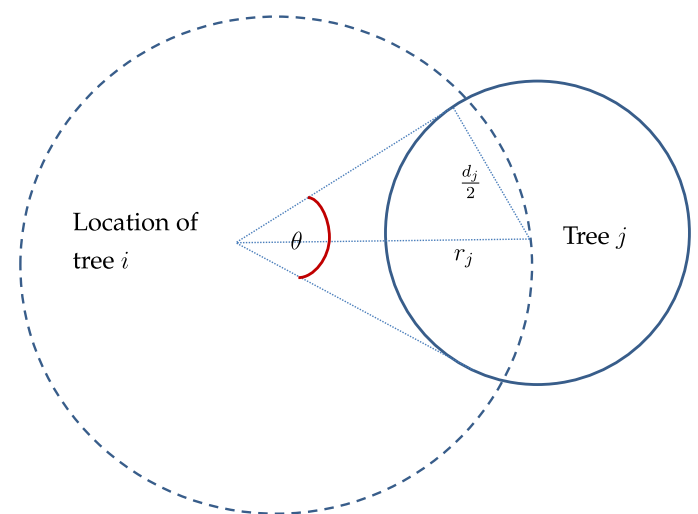

Fig. 1. The principle of individual-tree basal-area factors. d_j – stem diameter of tree *j* at 1.3 m above soil level, r_j – Euclidean distance between tree *j* and tree *i*, θ - angle based on the stem-diameter range of the trees to be sampled.

suggesting that Eq. (3) might form the basis of a new kernel function. Using the kernel notation of Pommerening and Grabarnik (2019, Chapter 5.2.2), the individual-tree basal-area factor in Eq. (3) was modified to yield a kernel function (Eq. (4)) as:

$$g_j(d_j, \, \xi) = \left(\frac{d_j}{1 + 2 \, dist_j(\xi)} \right)^\alpha, \tag{4}$$

where $g_j(d_j, \, \xi)$ is the *relascope kernel function* at an arbitrary location ξ in the forest related to tree j, which has a diameter d_j and is located at distance $dist_j(\xi)$ from ξ. From a theoretical point of view, Eq. (4) constitutes a *hyperbolic* or *fractional* interaction kernel (Adler, 1996; Schneider et al., 2006; Pommerening and Grabarnik, 2019, Chapter 5). Similar to the definition of other hyperbolic or fractional kernels, the addition of 1 in the denominator ensures that Eq. (4) is defined for $dist_j(\xi) = 0$, that is, at the location of tree j. The power 2 in Eq. (3) has been replaced by a general model parameter, α; this parameter is interpretable and controls both the *strength* and *range* of the kernel function as illustrated in Fig. 2A.

A similar, but more sophisticated kernel function is the exponential kernel,

$$g_j(d_j, \, \xi) = d_j^\alpha \times e^{\left\{ -\frac{\delta \cdot dist_j(\xi)}{d_j^\beta} \right\}}, \tag{5}$$

that has been used successfully in previous studies Pommerening et al., 2011; Pommerening and Maleki, 2014). In Eq. (5), parameter α controls the strength of the interaction signal expressed by the kernel function whilst β and δ define its range (Fig. 2A). The general shape of both kernel functions described in Eqs. (4) and ((5) is very similar, but the exponential kernel has three times the number of parameters of the relascope kernel. Following the terminology of Pommerening and Grabarnik (2019), Eqs. (4) and (5) are not strictly speaking kernel functions, which have a maximum value of one, but instead are *local effects* based on kernel functions; for simplicity we retain the term kernel function here.

2.2. Estimating growth rates based on kernel functions

One of the main benefits of the use of kernel functions in modelling is that their values for all the trees of a population can be aggregated multiplicatively or additively at any point ξ in the forest stand. This ultimately results in an interaction field Fig. 2B) that changes with time as trees grow, produce offspring and die and covers the whole horizontal extent of the forest stand (Pommerening et al., 2011; Pommerening and Grabarnik, 2019). The ultimate goal of producing an interaction field is also the reason why Eqs. (4) and ((5) include information only of those trees j that 'emit' interaction signals and not of those that are on the receiving end, that is, the subject trees i. This interaction field can now be employed in a second step to extract the amount of interaction each tree i faces at its own location. Of course, this modelling focus uses only a small, discretised fraction of the information that the interaction field offers. The whole field provides much more information and can, for example, be used also to estimate the probability of occurrence of processes such as tree mortality or tree regeneration. In those cases, it seems reasonable to assume that trees are more likely to die and less likely to regenerate where the intensity of the interaction field is high (Pommerening et al., 2021). As such, the interaction field can also be interpreted as a kind of resource map describing, for example, light, water or nutrient availability. When using the relascope kernel the resulting interaction field is also an approximate estimator of tree basal area at any point in the forest.

Tree growth depends mainly on the size of each tree, but also on its interaction with other trees which influence the availability of resources, such as light, water and nutrients Burkhart and Tomé, 2012; Weiskittel et al., 2011). The interaction load to which each subject tree i is exposed at its location ξ_i can be calculated as the additive aggregation of the interaction effects imposed ('emitted') by all other trees, $j \neq i$. Trees that are large and close to subject tree i naturally make a larger contribution to this interaction load than trees that are smaller and/or further way. The contribution of trees j that are very far from a subject tree is zero or near zero, therefore no explicit selection of competitors is required. The sum of interaction kernel values at ξ_i at any time, t, forms the interaction function, $H_{i,t}$, which is an expression of the interaction load tree i is facing at that time. To allow for asymmetric interaction it is advisable to divide the sum of interaction kernel values by the maximum kernel value at the location of tree i, which for both kernel types is d_i^α, since $dist_i(\xi_i) = 0$. Adding t as the temporal index to the terms of $g_j(d_j, \, \xi)$ of Eqs. (4) and ((5) yielded

$$H_{i,t} = \sum_{j \neq i} \frac{g_{j,t}(\xi_i)}{d_{i,t}^\alpha}. \tag{6}$$

To ensure that the values of the interaction function lie between 0 and 1 a further transformation was carried out (Häbel et al., 2019) to
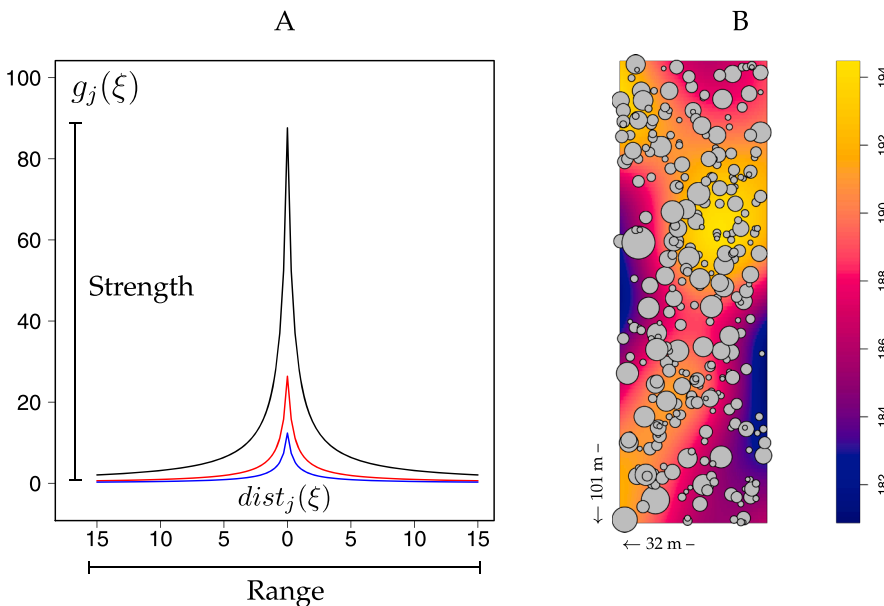

Fig. 2. Relascope kernel for trees with a stem diameter, d, of 60 (black), 20 (red) and 10 (blue) cm (A) and the corresponding interaction field for *Eucalyptus obliqua* plot 8009 at age 45 (B). The tree locations were indicated by grey filled circles which have diameters proportional to the diameters of the trees. Kernel parameter $\alpha = 1.09247$ (see Table 1) estimated from the *E. obliqua* data of plot 8009. Relative growth rate (RGR) was the dependent growth variable here. (For interpretation of the references to colour in this figure, the reader is referred to the web version of this article).

give $H_{i,t}^*$ in place of $H_{i,t}$ as

$$H_{i,t}^* = 1 - e^{\frac{\nu}{H_{i,t}}}, \tag{7}$$

which introduces another model parameter, ν.

In this study, we had data available from tree plots that differed both in the number of times each was measured and the interval between measurements. Accordingly we calculated the growth rate of an individual tree as the difference between its sizes at two measurements divided by the length of the time period between them. Growth rates were considered in stem diameter (d) and basal area ($g^* = \pi(d/2)^2$) and both of these in terms of their absolute and relative growth rates, AGR and RGR, respectively. In the following equations we refer to a general growth variable y, which can be either d or g^*. In tree modelling, basal-area growth rates are often preferred to stem-diameter growth rates as response or dependent variables, although evidence for the superiority of one of these growth rates is not substantial (West, 1980). The absolute growth rate, $\Delta y_{i,t}$, can be estimated as

$$\Delta y_{i,t} = \Delta y_{i,t}^{\text{pot}} \times H_{i,t}^*, \tag{8}$$

where $\Delta y_{i,t}^{\text{pot}}$ is the stem-diameter or basal-area growth potential that a tree would have, if competitive effects from other trees were absent. Eq. (8) is based on the hypothesis that the interaction load exerted on a tree by other trees in the stand reduces its growth rate from what it might potentially be. When basal area was used for y, stem-diameter AGR was derived from basal-area AGR through

$$\Delta d_{i,t} = 2 \times \sqrt{\frac{\Delta g_{i,t}^*}{\pi}} \tag{9}$$

In the RGR case, a few transformation steps (Eqs. (10)–(12)) need to be taken when basal area is used for y. Related to basal area at the beginning of the annual growth period, the upper bound of relative growth rate of basal area, $p_{i,t}^{+(g)}$, can be calculated as

$$p_{i,t}^{+(g)} = \frac{\Delta g_{i,t}^*}{g_{i,t-1}^*} \tag{10}$$

and logarithmic RGR, $p_{i,t}^{(g)}$, as commonly used in plant science

(Pommerening and Grabarnik, 2019, p. 264), can be obtained from $p_{i,t}^{+(g)}$ through

$$p_{i,t}^{(g)} = \log\left(1 + p_{i,t}^{+(g)}\right). \tag{11}$$

Finally, stem-diameter RGR is calculated from basal-area RGR using Eq. (12) (Sumida et al., 1997).

$$p_{i,t}^{(d)} = \frac{p_{i,t}^{(g)}}{2} \tag{12}$$

Potential growth as applied in Eq. (8) was determined from all the data we had available for each of the eight tree species sites we considered and was modelled using the Hugershoff function (Hugershoff, 1936 Zeide, 1993;, Eq. (7)):

$$\Delta y_{i,t}^{\text{pot}} = k \times y_{i,t}^p \times e^{-q \times y_{i,t}} \tag{13}$$

The parameters of the Hugershoff function were estimated as an upper quantile of absolute stem-diameter or basal-area growth (see Section 2.3) and as a function of y. k, p and q are the model parameters (Häbel et al., 2019, Fig. 3).

2.3. Estimation and validation characteristics

For parameter estimation of the various functions being considered here, we largely followed the methods described by Häbel et al. (2019). Firstly, we estimated the parameters k, p and q of the potential stem-diameter or basal-area growth model (Eq. (13)) for each data set. This was done applying quantile regression (Koenker and Park, 1994; Cade and Noon, 2003; West, 2021) with the quantile set to $\tau = 0.975$ as shown for examples in Fig. 3.

Secondly, the kernel parameters α (relascope kernel, Eq. (4)), α, β, δ (exponential kernel, Eq. (5)) and growth parameter ν (Eq. (7)) were estimated simultaneously through regression using stem-diameter/basal-area potential and tree interaction as independent (predictor) variables. Mean annual stem-diameter/basal-area RGR and AGR served as dependent (response) variable. As in Häbel et al. (2019), we applied both (weighted) nonlinear least-squares and maximum-likelihood approach for estimating kernel and growth parameters. We checked various goodness-of-fit characteristics including the distribution of $H_{i,t}^*$, the residuals and the shape of the interaction kernels to select the best
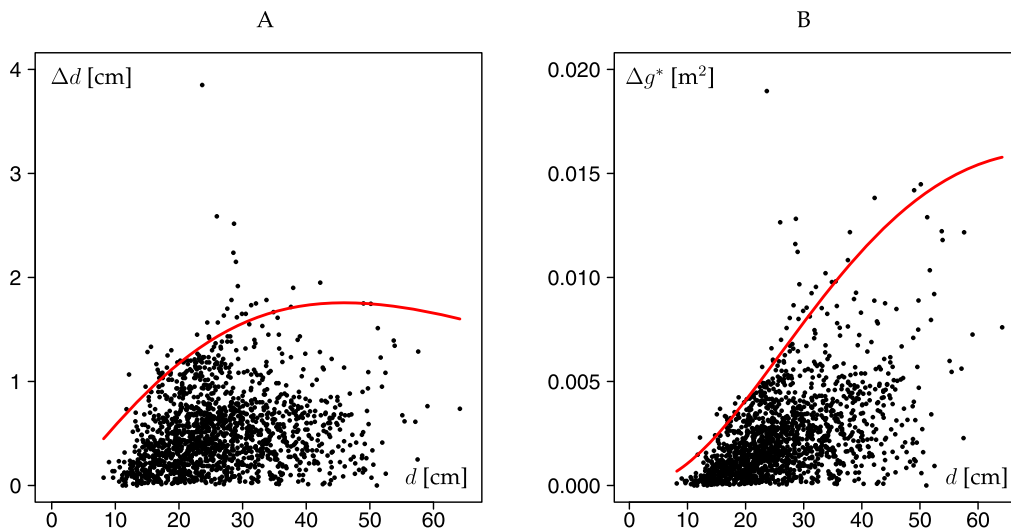
Fig. 3. Stem-diameter, $\Delta d_{i,t}$, (A) and basal-area, $\Delta g_{i,t}^*$, (B) absolute growth-rate potentials (red curves) estimated from stem diameter, d, at the start of the growth period concerned and using quantile regression with $\tau = 0.975$ for *Pinus pinaster* (Galicia, Spain). (For interpretation of the references to colour in this figure, the reader is referred to the web version of this article).

estimation for each data set. In the regression, we applied periodic boundary conditions (Pommerening and Grabarnik. 2019, p. 177) for spatial edge correction.

For evaluating the regression results we quantified common characteristics such as bias and RMSE (root mean square error). These characteristics always related to stem diameter. In addition and for better comparison between data sets we calculated *relative bias* and *efficiency*. Relative bias, *B*, is defined as

$$B = \frac{\sum_{i=1}^{n}(\widehat{y}_i - y_i)}{n\overline{y}}, \tag{14}$$

where $\widehat{y}_i$ is the *i*th prediction (modelled stem-diameter AGR or RGR), y_i is the *i*th observation (observed stem-diameter AGR or RGR), n is the number of observations and $\overline{y}$ is the mean observation. Efficiency, *E*, is defined as

$$E = 1 - \frac{\sum_{i=1}^{n}(\widehat{y}_i - y_i)^2}{\sum_{i=1}^{n}(y_i - \overline{y})^2}. \tag{15}$$

Efficiency values approach 1 with improving model performance. A value of zero indicates that the model explains no more variation than the mean value of the observations alone and negative values highlight biased estimates. For this analysis we used our own R (R Development Core, Team, 2020) and C++ code.

2.4. Study data

Spatially explicit time-series data from three plots of three eucalypt species were included in this study. They were originally measured as part of a collation of eucalypt data from Australian forest agencies (Mattay and West, 1994). All three plots had been established in even-aged, monoculture re-growth forests in Tasmania. Plot 8009 (146°54′ E, 43°24′ S) included *Eucalyptus obliqua* L'Hér, regenerated in 1920, contained 337 trees at 39 years of age and was then re-measured on six occasions at 1–5 year intervals. Plot 8055 (147°53′ E, 43°04′ S) was of *E. regnans* F. Muell. and regenerated in 1940, had 535 trees at 15 years of age and was re-measured seven times at 3–4 year intervals. Plot 4000 (147°40′ E, 41°25′ S) was of *E. delegatensis* R. Baker. The trees regenerated in 1950, had 126 trees at 29 years of age and was re-measured four times at 2–3 year intervals. For this study, the data from all three plots were analysed separately.

Data of European beech (*Fagus sylvatica* L.) were collected in a total of 17 plots of varying size at each of the five different sites at Aarburg, Concise, Embrach, Zofingen and Zollikon in the Jura region, the Swiss plains and the Pre-Alps. These plots are part of a long-term monitoring network dedicated to studying growth dynamics of *F. sylvatica* and are located at altitudes below 800 m a.s.l. The time series had 4–9 re-measurements at variable survey intervals with an average of 7 years and were located in pure and even-aged *F. sylvatica* forests (Álvarez-González et al., 2010; Pommerening et al., 2021). For this study, the data from all 17 plots were pooled.

Norway spruce (*Picea abies* (L.) Karst.) spatio-temporal data were recorded in 16 plots (30 m × 40 m each) at Karlstift in Austria (14°46′ E, 48°35′ N) with three re-measurements. Originally, the plots were part of a replicated thinning experiment. The plots were located at 930 m a.s.l., with a mean annual temperature of 4.5 °C and a mean annual precipitation of 950 mm. They were established in 1964 in predominantly even-aged *P. abies* that had regenerated naturally and were re-measured every five years until 2004 (Pommerening et al., 2011). For this study, the data from all 16 plots were pooled.

Interior Douglas fir (*Pseudotsuga menziesii* var *glauca* (Mirb.) Franco) data were collected from an uneven-aged stand in the Alex Fraser Research Forest in British Columbia, Canada (121°52′ W, 52°3′ N) at approximately 1000 m a.s.l. The mean annual temperature was 4.2 °C and the mean annual precipitation was 450 mm. The data were measured in six plots starting in 1988 with re-measurements in 1992,

1997 and 2004. Four plots were 0.10 ha in area and two, with higher tree densities, were of 0.05 ha. The forest site had not been cut for at least 20 years and was protected from large-scale fires (LeMay et al., 2009; Häbel et al., 2019). For this study, the data from all 6 plots were pooled.

The Atlantic maritime pine forests of *Pinus pinaster* Aiton are of great productive and ecological importance in northwestern Spain. The species covers 15.4% of the forest area in Galicia. *P. pinaster* is native to the area and is also grown in plantations with rotation periods of 30–40 years. The species usually regenerates naturally and prolifically after clear-felling and is well adapted to forest fire ecosystems. Twenty four plots of 25 m × 40 m were installed in 2006 in old stands of *P. pinaster* throughout Galicia and were re-measured twice in 2007 and 2009. The plots were located in community forests and were chosen to include the natural range of the species. The mean air temperature ranges from 10.4 °C to 12.9 °C in the region, and the mean annual rainfall is 1392 mm. Elevation ranges from 325 m to 773 m a.s.l (Eimil Fraga, 2016). For this study, the data from all 24 plots were pooled.

Our study also included Scots pine (*Pinus sylvestris* L.) data from two monitoring plots in the remnants of the Caledonian pinewoods, namely Abernethy and 'young' Glenmore (Queens 26, plot 5) UK (4°15′ W, 57°30′ N). For several millennia, vast areas of northern Scotland were once covered by the Caledonian pinewoods. The forest sites are situated at approximately 330 m a.s.l. Mean annual rainfall is 900 mm and mean annual temperature about 6.0 °C. Abernethy represents a well-structured old-growth, natural forest. It was first measured in 2002 and then re-measured in 2008 on a 0.8-ha plot. 'Young' Glenmore was planted in 1926 to replace an old stand felled during World War I. The forest was first measured in 2003 and subsequently re-measured in 2008, 2013 and 2018 on a 1-ha plot (Mason et al., 2007; Häbel et al., 2019). For this study, the data from the two plots were pooled.

For convenience we have used the prevailing species name when referring to each data set hereafter.

3. Results

3.1. Growth potentials

An important outcome of this work is the finding that the growth potential had considerable influence on the estimation of the parameters of the kernel function. For estimating *relative growth rates* it was, in terms of the performance criteria described in Section 2.3, usually found best to define the growth potentials based on *basal-area* AGR. For estimating *absolute growth rates* it was generally only possible to define growth potential in terms of *stem-diameter* AGR, since the regressions involving the kernel functions when based on potential basal-area AGR would in that case not yield realistic model parameters, in terms of the performance criteria described in Section 2.3. With both modelling alternatives, the independent variable of the growth-potential estimation was stem diameter (Fig. 3). It has also proved advantageous, and made the model more versatile, to always model AGR growth potentials rather than RGR potentials irrespective of whether AGR or RGR was the final dependent variable in the regression. RGR-dbh point clouds often differed substantially in shape from the data set of one species to that of another, whilst AGR-dbh point clouds (as in Fig. 3) largely shared the same shape and their quantile data were amendable to being described by the same general model (Eq. (13)).

3.2. Correlations between growth rates and individual-tree basal-area factors

Individual-basal area factors (Eq. (3)) formed the starting point of our modelling work. Consequently, as a preparation for modelling, we studied the relationship between individual-basal area factors and relative and absolute growth rates. More specifically, as an expression of competition load and in analogy to Eq. (6) we calculated the sum of

individual-basal area factors over all trees other than subject tree *i*. Finally we divided this sum by the square of stem diameter of tree *i* to obtain a measure of asymmetric competition, i.e.

$$H_{i,t}^{(\beta^*)} = \frac{\sum \beta_i^*}{d_i^2}. \tag{16}$$

$H_{i,t}^{(\beta^*)}$ and both RGR/AGR were negatively correlated, i.e. small growth rates occurred more where values of $H_{i,t}^{(\beta^*)}$ were large (Fig. 4). Both the RGR and AGR point clouds greatly varied from study site to study site. For small trees RGR is usually largest. The *E. regnans* data (Fig. 4Ca) showed the largest and *F. sylvatica* (Fig. 4Cb) the smallest relative growth rates.

Some RGR point clouds had a larger vertical and horizontal spread than others. The point clouds related to the *P. abies* plots (Fig. 4Ac), for example, had a comparatively large horizontal spread and the point cloud of *E. regnans* (Fig. 4Ca) showed a large vertical spread. Noteworthy is the almost uniform distribution of RGR in the natural *P. menziesii* forest (Fig. 4Cc).

The AGR point-cloud patterns were in fact not too dissimilar from the RGR patterns. Also here, the general pattern was that of a (negative) exponential distribution. When comparing AGR and RGR, the tendency to this distribution was for some data stronger for AGR than for RGR for some data, e.g. *P. abies* plots (Fig. 4Bc, 4Ac), *F. sylvatica* (Fig. 4Db, 4Cb)
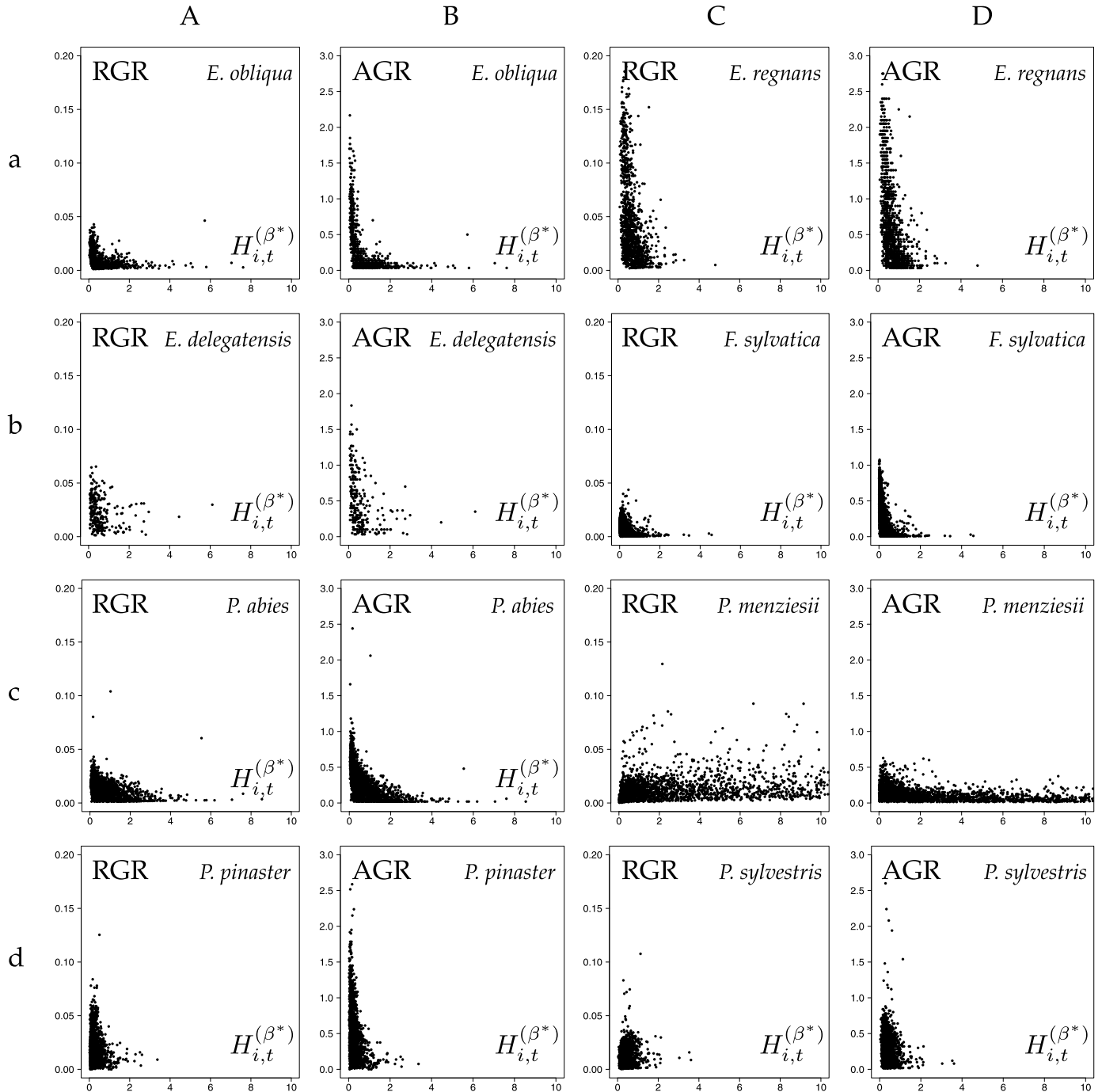

Fig. 4. Point clouds of mean annual relative (RGR) and absolute (AGR) growth rates over $H_{i,t}^{(\beta^*)}$ (Eq. (16))..

and *P. menziesii* forest (Fig. 4Dc, 4Cc). Yet, for other data, there was hardly any difference in the point-cloud shapes between AGR and RGR, e.g. *E. regnans* (Fig. 4Da, 4Ca), *P. pinaster* (Fig. 4Bd and Fig. 4Ad) and *P. sylvestris* (Fig. 4Dd, Fig. 4Cd).

Based on these initial results involving $H_{i,t}^{(\beta^*)}$ we hypothesised that the relascope kernel function performed best with those data where the RGR or AGR point clouds most closely exhibited an exponential pattern.

3.3. Regression results

Regressions for both the relascope and the exponential kernels with regard to RGR as the dependent variable were determined satisfactorily for all eight data sets (Table 1). As expected, usually the use of exponential kernels with three model parameters instead of one led to greater efficiencies than the application of relascope kernels. However, the differences were often moderately large, e.g. in the case of *E. obliqua* (20.5% gain), *F. sylvatica* (29.8% gain), *P. abies* (4.0% gain) and *P. sylvestris* (20.1% gain). The largest gain achieved by applying the exponential kernel instead of the relascope kernel was 47.2% for *E. regnans*.

These gains came at the expense of two more model parameters and greater estimation difficulties. In the majority of cases acceptable regression results were more straightforward to obtain for the relascope kernel, i.e. the regression was more robust. Estimation difficulties were often indicated by very large and very small model parameters (α, β, δ, ν). With the relascope kernel this was the case for *P. menziesii* and parameter ν. With the exponential kernel this situation occurred for δ with *E. obliqua*, *E. regnans* and *P. pinaster*. With the exponential kernel there was also a very small value for β with *E. delegatensis*. In four out of eight cases the absolute relative bias, *B*, (Eq. (14)) was smaller when the relascope kernel was applied rather than the exponential kernel.

Using stem-diameter AGR potentials, the same regressions were also possible for AGR as the dependent variable (Table 2). The efficiency values were generally considerably higher in Table 2 than in Table 1.

This result was consistent with our earlier observations made concerning Fig. 4, i.e. our hypothesis stating that the performance of the relascope kernel can be anticipated from the point clouds in Fig. 4 is true. The AGR point cloud often followed the shape of an exponential distribution more than the RGR point cloud and with AGR there was usually less of a concentration of points near the origin of the system of coordinates. In Table 2, we also noted the same efficiency trend as for

RGR in Table 1, i.e. the efficiencies were usually markedly higher for the exponential kernel. For *E. obliqua*, *E. delegatensis* and *P. abies* the gain of using an exponential kernel instead of a relascope kernel was 14.9%, 6.3% and 7.2%, respectively. These percentages are generally lower than the minimum percentages calculated from Table 1. For *P. pinaster* and *P. sylvestris* this gain exceeded 100%. These large differences were attributed to the fact that the efficiencies for the two pine data sets were negative for the relascope kernel. The gains achieved by the exponential kernel were again contrasted by the much larger number of parameters in the exponential kernel and the associated estimation difficulties. With the relascope kernel, suspiciously large ν values occurred only for *P. menziesii* and *P. sylvestris*. By contrast, with the exponential kernel a suspicious β value was obtained for *E. delegatensis*. In addition, large δ and/or ν values were estimated for *E. obliqua, E. regnans, P. pinaster* and *P. sylvestris*. Only the absolute relative bias, *B*, associated with the relascope kernel and *P. menziesii* was smaller than that achieved with the exponential kernel.

4. Discussion and conclusions

Neighbourhood interactions are an important process in plant population dynamics and the quantification of such processes is therefore a core interest of quantitative forest ecology (Schneider et al., 2006; Berger and Hildenbrandt, 2000; Häbel et al., 2019).

Individual-tree basal-area factors and relascope kernel functions are comparatively simple quantities that can play important roles both in forest ecology and resource management (Rouvinen and Kuuluvainen, 1997; McTague, 2010; McTague and Weiskittel, 2016; Stage and Ledermann, 2008). Resource managers, forest practitioners and forest scientists are very familiar with the relascope concept which eases the understanding and application of these techniques in individual-based modelling. By using measures forest practitioners and resource managers are familiar with, trust in new models and the applications can be inspired.

After analysing data from eight very different forest ecosystems located in different parts of the world, our work demonstrated that the relascope kernel function can indeed be applied in individual-based models like any other kernel function and thus achieve a generalisation of individual-tree basal area factors. Relascope kernels can be even used for estimating two different growth rates, relative and absolute growth rates, as dependent or response variables. Such a comparison of

Table 1

Synopsis of the site and model specific parameters and statistical characteristics related to RGR. For *P. pinaster* the parameters of the stem-diameter growth potential (left) were used for the relascope kernel and the parameters of the basal-area growth potential (right) were applied in connection with the exponential kernel. For *P. sylvestris* and both kernel functions the stem-diameter growth potential was applied. For all other data sets basal-area growth potentials were used throughout. RMSE – root mean square error, Bias – bias, AIC – Akaike information criterion. Other symbols are explained in the text.

Model	Model parameter	*E. obliqua*	*E. regnans*	*E. delegatensis*	*F. sylvatica*	*P. abies*	*P. menziesii*	*P. pinaster*		*P. sylvestris*
Potential	k	1.04010e-07	0.00025	1.04823e-06	2.59228e-06	4.96050e-07	0.00003	0.031	0.000	0.10740
	p	3.36593	1.22651	3.04996	2.21458	3.04781	1.40631	1.445	2.433	0.65553
	q	0.02751	0.04477	0.04526	0.01374	0.04340	0.02342	0.034	0.034	0.01024
Relascope kernel	α	1.09247	2.30858	1.38878	1.45426	1.48721	0.38388		1.54483	1.22863
	ν	1.70853	0.07953	0.56621	0.31304	0.90939	16.50000		0.00059	0.00404
	RMSE	0.00628	0.01688	0.01450	0.00449	0.00639	0.01508		0.01281	0.00901
	Bias	−0.00081	0.00116	−0.00491	0.00007	−0.00058	−8.98951e-06		0.00005	0.00030
	AIC	−8298.96	−22,270.37	−1261.49	−36,806.53	−46,597.88	−13,294.62		−9751.39	−17,189.02
	B	−0.10203	0.05457	−0.22372	0.00844	−0.04424	−0.00066		0.00244	0.02778
	E	0.30529	0.47600	0.04077	0.27062	0.40359	0.18308		0.17413	0.09526
Exponential kernel	α	1.23235	3.56463	0.25131	1.26328	0.89773	0.18308		0.83534	0.83792
	β	1.58414	1.92299	2.05049 e-16	0.62516	0.60985	0.14830		1.31162	0.27224
	δ	47.65857	67.41743	0.30731	2.17004	3.66575	0.85043		27.93016	0.24686
	ν	4.21054	3.25650	2.00674	1.58203	1.10079	1.14914		1.22039	0.03153
	RMSE	0.00595	0.01134	0.01437	0.00419	0.00630	0.01395		0.01143	0.00891
	Bias	−0.00115	−0.00055	−0.00438	0.00015	−0.00010	−0.00004		−0.00008	0.00013
	AIC	−15,638.02	−24,406.58	−3069.26	−61,245.71	−46,721.89	−29,092.11		−17,384.10	−26,423.92
	B	−0.14504	−0.02568	−0.19965	0.01949	−0.00770	0.00314		−0.00405	0.01240
	E	0.37493	0.76338	0.05698	0.36462	0.42015	0.30123		0.34283	0.11642

Table 2

Synopsis of the site and model specific parameters and statistical characteristics related to AGR. Throughout this table stem-diameter growth potentials were applied. RMSE – root mean square error, Bias – bias, AIC – Akaike information criterion. Other symbols are explained in the text.

Model	Model parameter	*E. obliqua*	*E. regnans*	*E. delegatensis*	*F. sylvatica*	*P. abies*	*P. menziesii*	*P. pinaster*	*P. sylvestris*
Potential	k	0.00071	0.33446	0.00638	0.00590	0.00055	0.16251	0.03110	0.10740
	p	2.32845	0.94344	2.05600	1.57251	2.81359	0.47387	1.44457	0.65553
	q	0.02655	0.07744	0.04685	0.02257	0.07220	0.02373	0.03395	0.01024
Relascope kernel	α	0.94000	2.07120	0.85658	1.32948	0.09101	0.39830	1.05254	0.74470
	ν	3.26186	0.17114	3.90138	0.49589	5.29119	20.37018	1.18739	14.93404
	RMSE	0.19892	0.27510	0.28742	0.15026	0.13700	0.07939	0.39387	0.24468
	Bias	−0.00849	0.02677	−0.00558	−0.00753	−0.01414	0.00463	−0.04905	−0.01604
	AIC	−511.15	623.86	99.37	−21,220.53	−4481.32	−17,344.09	−3836.37	64.37
	B	−0.03432	0.07931	−0.01209	−0.02811	−0.04723	0.00463	−0.10003	−0.05944
	E	0.59227	0.40178	0.42177	0.46682	0.62834	0.30826	−0.06017	−0.11565
Exponential kernel	α	1.12332	3.34105	0.72003	1.13401	0.49041	0.27811	0.91807	0.47353
	β	3.06762	2.05713	1.05320e-14	0.77532	0.92425	0.50187	1.46278	1.87187
	δ	6.58605e+47	105.73381	0.25688	3.32263	7.98963	2.31956	36.31561	36.04240
	ν	18.130212	3.66457	4.12447	2.38279	2.09311	1.23327	2.35835	34.68698
	RMSE	0.17405	0.17156	0.28047	0.13602	0.12807	0.07133	0.31893	0.21812
	Bias	0.00483	0.00494	0.00042	0.00370	0.00608	0.00318	0.00475	0.00110
	AIC	−5464.81	−9780.90	−977.74	−22,329.39	−19,329.98	−18,063.80	−4640.26	−8635.59
	B	0.01954	0.01463	0.00091	0.01382	0.02029	0.03221	0.00968	0.00406
	E	0.68784	0.76734	0.44940	0.56305	0.67524	0.44162	0.30488	0.11337

performance with different growth rates as response variables does not appear to have been done previously. By plotting these growth rates over the values of the interaction function constructed from individual-tree basal-area factors (Eq. (16), Fig. 4) it is even possible to anticipate the performance and suitability of the relascope kernel for a given data set; this should save the analyst from spending time and effort on modelling what would eventually yield poor results. As expected, growth rates and the interaction function $H_{i,t}^{(\beta^*)}$ were negatively correlated, i.e. large values of $H_{i,t}^{(\beta^*)}$ typically lead to a reduction of growth rates.

When comparing the relascope kernel with the exponential kernel as a reference, it turned out that the behaviour of the relascope kernel was usually more robust in regressions. Judging by the efficiency results, the exponential kernel, however, was more exact in modelling the interaction field, although earlier research has shown that the difference in attenuation with distance as a result of using different kernel functions plays a rather minor role (Schneider et al., 2006). Both performance aspects are related to the difference in the number of model parameters.

Considering the very different data sets involving eight tree species, greater efficiencies (Eq. (15)) could in most cases be achieved when AGR was used as dependent variable. In that case the efficiency differences were also smaller between relascope and exponential kernel function than in a situation where RGR was the dependent variable. However, there were also situations where the RGR model outperformed the AGR model, such as in the case of the *E. regnans, P. pinaster* and *P. sylvestris* data (Table 1 and 2) and, again, scatter plots such as those in Fig. 4 can aid the decision process. Therefore the final choice of RGR versus AGR as dependent variable in the regression always depends on the actual data at hand and on the objectives of modelling.

An interesting and helpful result of our study was the discovery of a clear and strong influence of the potential-growth model on the parameters of the kernel function: In the case of stem-diameter AGR, reliable parameters of the two kernel functions could only be estimated, when the growth potential (Eq. (13)) was based on stem-diameter AGR as well. By contrast, when stem-diameter RGR was the dependant variable, the regressions led in most cases to more reliable parameters of the two kernel functions if the growth potential was based on basal-area AGR. In the same way, the finding that the modelling process is more straightforward when potential growth is generally based on AGR, even if RGR is the dependent variable of the regression, may prove helpful in future modelling work; this influence of the growth potential needs to be considered in future modelling efforts.

Kernel functions play a crucial role in individual-based modelling where they are used to model interaction, birth and sometimes even death processes. Our study has shown that simple, parsimonious functions such as the relascope kernel can be quite effective and an important starting point for quantifying the interaction dynamics in forest ecosystems.

Data accessibility statement

The data and the analysis R/C++ code used in this study are available at https://zenodo.org/record/6299823 or using DOI 10.5281/zenodo.6299823.

Credit author statement

All authors analysed the data, carried out the analyses and substantially contributed to the text. All persons entitled to co-authorships have been included in this paper. All authors have seen and approved the submitted version of the manuscript.

Declaration of Competing Interest

The authors declare that they have no known financial interests or personal relationships that could have influenced the work reported in this paper.

References

Adler, F.R., 1996. A model of self-thinning through local competition. Proc. Natl. Acad. Sci. U.S.A. 93, 9980–9984.

Álvarez-González, J.G., Zingg, A., Gadow, K.v., 2010. Estimating growth in beech forests: a study based on long-term experiments in Switzerland. Ann. For. Sci. 67, 307.

Berger, U., Hildenbrandt, H., 2000. A new approach to spatially explicit modelling of forest dynamics: spacing, ageing and neighbourhood competition of mangrove trees. Ecol. Modell. 132, 287–302.

Binkley, D., 2004. A hypothesis about the interaction of tree dominance and stand production through stand development. For. Ecol. Manag. 190, 265–271.

Bitterlich, W., 1984. The Relascope Idea. Relative Measurements in Forestry. Commonwealth Agricultural Bureaux, Norwich.

Burkhart, H.E., Tomé, M., 2012. Modeling Forest Trees and Stands.

Cade, B.S., Noon, B.R., 2003. A gentle introduction to quantile regression for ecologists. Front. Ecol. Environ. 1, 412–420.

Daniels, R.F., 1976. Simple competition indices and their correlation with annual loblolly pine tree growth. For. Sci. 22, 454–456.

Eimil Fraga, C., 2016. Analysis of the Edaphic and Ecophysiological Parameters in Relation to Nutrient Levels and Growth of *Pinus pinaster* in Acidic Soils. PhD Thesis University of Santiago de Compostela, Lugo.

Gadow, K.v., Hui, G., 1999. Modelling Forest Development. Springer, Dordrecht.

Green, E.J., 1992. Forest growth with point sampling data. Conserv. Biol. 6, 296–297.

Gregoire, T.G., Valentine, H.T., Furnival, G.M., 1995. Sampling methods to estimate foliage and other characteristics of individual trees. Ecology 76, 1181–1194.

Gregoire, T.G., 1998. Design-based and model-based inference in survey sampling: appreciating the difference. Can. J. For. Res. 28, 1429–1447.

Gregoire, T.G., Schabenberger, O., 1999. Sampling-skewed biological populations: behaviour of confidence intervals for the population total. Ecology 80, 1056–1065.

Gregoire, T.G., Valentine, H.T., 2008. Sampling Strategies for Natural Resources and the Environment. Chapman & Hall/CRC, Boca Raton.

Grosenbaugh, L.R., 1952. Plotless timber estimates – new, fast, easy. J. For. 50, 32–37.

Häbel, H., Myllymäki, M., Pommerening, A., 2019. New insights on the behaviour of alternative types of individual-based tree models for natural forests. Ecol. Modell. 406, 23–32.

Hugershoff, R., 1936. Die mathematischen Hilfsmittel des Kulturingenieurs und Biologen. II. Teil: Herleitung von gesetzmäßigen Zusammenhängen. [Mathematical Tools for Forest Engineers and Biologists. Part II: Deriving relationships Based on Natural laws.] Dresden, unpublished manuscript.

Koenker, R., Park, B.J., 1994. An interior point algorithm for nonlinear quantile regression. J. Econom. 71, 265–283.

Krebs, C.J., 1999. Ecological Methodology, 2nd edition. Addison Wesley Longman, New York.

LeMay, V., Pommerening, A., Marshall, P., 2009. Spatio-temporal structure of multi-storied, uneven-aged interior Douglas fir (*Pseudotsuga menziesii* var *glauca* (Mirb.) Franco) stands. J. Ecol. 97, 1062–1074.

Lorimer, C.G., 1983. Tests of age-independent competition indices for individual trees and natural hardwood stands. For. Ecol. Manag. 6, 343–360.

Mason, W.L., Connolly, T., Pommerening, A., Edwards, C., 2007. Spatial structure of semi-natural and plantation stands of Scots pine (*Pinus sylvestris* L.) in northern Scotland. Forestry 80, 567–586.

Mattay, J.P., West, P.W., 1994. A collection of growth and yield data from eight eucalypt species growing in even-aged monoculture forest. CSIRO Division of Forestry, User Series No 18. CSIRO, Canberra.

McTague, J.P., 2010. New and composite point sampling estimates. Can. J. For. Res. 40, 2234–2242.

McTague, J.P., Weiskittel, A.R., 2016. Individual-tree competition indices and improved compatibility with stand-level estimates of stem density and long-term production. Forests 7, 238.

Montgomery, D.C., 2013. Design and Analysis of Experiments, 8th edition. John Wiley & Sons, New Delhi.

Motz, K., Sterba, H., Pommerening, A., 2010. Sampling measures of tree diversity. For. Ecol. Manag. 260, 1985–1996.

Newton, A.C., 2007. Forest Ecology and Conservation. A Handbook of Techniques. Oxford University Press, Oxford.

Ouyang, S., Xiang, W., Wang, X., Xiao, W., Chen, L., Li, S., Sun, H., Deng, X., Forrester, D. I., Zeng, L., Lei, P., Lei, X., Gou, M., Peng, C., 2019. Effects of stand age, richness and density on productivity in subtropical forests in China. Ecology 107, 2266–2277.

Pommerening, A., LeMay, V., Stoyan, D., 2011. Model-based analysis of the influence of ecological processes on forest point pattern formation – a case study. Ecol. Modell. 222, 666–678.

Pommerening, A., Maleki, K., 2014. Differences between competition kernels and traditional size-ratio based competition indices used in forest ecology. For. Ecol. Manag. 331, 135–143.

Pommerening, A., Grabarnik, P., 2019. Individual-based Methods of Forest Ecology and Management. Springer, Cham.

Pommerening, A., Gaulton, R., Magdon, P., Myllymäki, M., 2021. CanopyShotNoise – an individual-based tree canopy modelling framework for projecting remote-sensing data and ecological sensitivity analysis. Int. J. Remote Sens. 42, 6837–6865.

Rasmussen, C.R., Weiner, J., 2017. Modelling the effect of size-asymmetric competition on size inequality: simple models with two plants. Ecol. Modell. 343, 101–108.

R Development Core Team, 2020. R: A Language and Environment for Statistical Computing. R Foundation for Statistical Computing, Vienna, Austria. http://www.r-project.org.

Rouvinen, S., Kuuluvainen, T., 1997. Structure and asymmetry of tree crowns in relation to local competition in a natural mature Scots pine forest. Can. J. Forest Res. 27, 890–902.

Schneider, M.K., Law, R., Illian, J., 2006. Quantification of neighbourhood-dependent plant growth by Bayesian hierarchical modelling. J. Ecol. 94, 310–321.

Spurr, S.H., 1962. A measure of point density. For. Sci. 8, 85–96.

Stage, A.R., Ledermann, T., 2008. Effects of competitor spacing in a new class of individual-tree indices of competition: semi-distance-independent indices computed for Bitterlich versus fixed-area plots. Can. J. For. Res. 38, 890–898.

Stöhr, K.F., 1959. Ein Vorschlag zur Erreichung einer höheren Genauigkeit bei Probeflächenaufnahmen nach der Winkelzählprobe. [A new method to achieve a greater accuracy in Bitterlich surveys.]. Allgemeine Forst- und Jagdzeitschrift 130, 23–29.

Sumida, A., Ito, H., Isagi, Y., 1997. Trade-off between height growth and stem diameter growth for an evergreen oak, *Quercus glauca*, in a mixed hardwood forest. Funct. Ecol. 11, 300–309.

Tomé, M., Burkhart, H.E., 1989. Distance-dependent competition measures for predicting growth of individual trees. For. Sci. 35, 816–831.

National forest inventories. In: Tomppo, E., Gschwantner, T., Lawrence, M., McRoberts, R.E. (Eds.), 2010. Pathways for Common Reporting. Springer, Dordrecht.

Weiskittel, A.R., Hann, D.W., Kerschaw, J.A., Vanclay, J.K., 2011. Forest Growth and Yield Modeling. Wiley Blackwell, Chichester.

West, P.W., 1980. Use of diameter increment and basal area increment in tree growth studies. Can. J. For. Res. 10, 71–77.

West, P.W., 2015. Tree and Forest Measurement, 3rd edition. Springer, Cham.

West, P.W., 2021. Modelling maximum stem basal area growth rates of individual trees of *Eucalyptus pilularis* Smith. For. Sci. 67, 633–636.

Zeide, B., 1993. Analysis of growth equations. For. Sci. 39, 594–616.